

# The role of spin-flip transitions in the anomalous Hall effect of FePt alloy

Hongbin Zhang, Frank Freimuth, Stefan Blügel, and Yuriy Mokrousov\*  
*Peter Grünberg Institut and Institute for Advanced Simulation,  
Forschungszentrum Jülich and JARA, D-52425 Jülich, Germany*

Ivo Souza  
*Centro de Física de Materiales and DIPIC, Universidad del País Vasco, 20018 San Sebastián, Spain and  
Ikerbasque, Basque Foundation for Science, E-48011 Bilbao, Spain*  
(Dated: October 18, 2018)

We carry out *ab initio* calculations which demonstrate the importance of the non-spin-conserving part of the spin-orbit interaction for the intrinsic anomalous Hall conductivity of ordered FePt alloys. The impact of this interaction is strongly reduced if Pt is replaced by the lighter isoelectronic element Pd. An analysis of the interband transitions responsible for the anomalous velocity reveals that spin-flip transitions occur not only at avoided band crossings near the Fermi level, but also between well-separated pairs of bands with similar dispersions. We also predict a strong anisotropy in the anomalous Hall conductivity of FePt caused entirely by low-frequency spin-flip transitions.

The intrinsic anomalous Hall effect (AHE) [1] and spin Hall effect (SHE) [2] in solids arise from the opposite anomalous velocities experienced by spin-up and spin-down electrons as they move through the spin-orbit-coupled bands under an applied electric field. In paramagnets, where the bands are spin-degenerate, these counter-propagating transverse currents result in a time-reversal conserving pure spin current. In ferromagnets, where the bands are split by the exchange interaction, the same process generates a net time-odd charge current.

The above picture is intuitively appealing, and often leads to correct conclusions. However, it leaves out the fact that in the presence of the spin-orbit interaction (SOI) the spin projection along the quantization axis is not a good quantum number. This is a particularly subtle point regarding the SHE, as the proper definition of the spin current becomes problematic when spin is not a conserved quantity [3]. More generally, processes which do not conserve spin (we shall refer to them as spin-flip processes) are known to play a role in phenomena such as spin relaxation [4] and magnetocrystalline anisotropy [5].

How does the lack of spin conservation affect the AHE? To analyze this issue, we begin by noting that the anomalous velocity results from virtual interband transitions, and that the matrix elements involved are the same which describe magnetic circular dichroism (see Eq. (1) below). In a perturbative expansion in powers of the spin-orbit coupling strength, the spin-conserving (spin-non-conserving) part of the SOI contributes to the dichroic conductivity at first (second) order [6]. The effect of spin-flip transitions is therefore expected to be comparatively small, as confirmed by recent tight-binding calculations of the anomalous Hall conductivity (AHC) for the *3d* transition metals [7].

It should be kept in mind, however, that in materials containing heavy atoms the SOI cannot be treated as a small perturbation. Moreover, first-principles calculations of the AHC [8] have established the crucial role of

near degeneracies across the Fermi level, for which the above arguments, based on non-degenerate perturbation theory, do not apply. While the full SOI was included in previous calculations [1], the specific role of the non-spin-conserving part was not thoroughly investigated.

In this Letter, we use first-principles calculations to study the impact of spin-flip transitions on the intrinsic AHC of FePt ordered alloys [9, 10]. This material has a number of desirable properties for the present study. Firstly, the heavy element Pt provides the strong SOI, which can be "tuned" by replacing Pt with Pd. Secondly, previous work has established that in samples with finite disorder the intrinsic contribution to the AHC is much larger than the extrinsic one [10]. It is becoming increasingly clear that the AHE in moderately resistive samples of itinerant ferromagnets such as FePt is often dominated by the intrinsic contribution [1], which at present is the only one that can be reliably calculated from first-principles in materials with unknown structural disorder and impurity content. We shall therefore focus exclusively on the intrinsic part of the AHC, neglecting extrinsic contributions such as skew-scattering and side-jump. We find that the contribution of spin-flip transitions to the AHC of FePt is considerable, amounting to about one fifth of the total value. More importantly, the calculations reveal a clear experimental signature of spin-flip transitions: as the magnetization is rotated from the uniaxial direction to the basal plane, their contribution to the AHC changes sign, leading to a factor-of-two reduction in the net AHC. In contrast, the spin-conserving part is almost perfectly isotropic.

We identify two distinct mechanisms for the spin-flip transitions. The first involves spin-orbit-induced avoided crossings at the intersections between exchange-split up- and down-spin Fermi-surface sheets (these intersections occur along lines in *k*-space which we shall refer to as *hot loops*, in analogy with the *hot spots* which have been discussed in connection with spin-relaxation in nonmagnetic

		$\sigma^{\text{tot}}$	$\sigma^{\uparrow\uparrow}$	$\sigma^{\uparrow\downarrow}$	$\Delta\sigma^{\uparrow\uparrow}$	$\Delta\sigma^{\uparrow\downarrow}$
FePt	[001]	818.1	576.6	133.4	-8.5	317.3
	[100]	409.5	585.1	-183.9		
FePd	[001]	135.1	108.4	28.4	-88.5	-33.6
	[100]	275.9	196.9	62.0		

TABLE I: Values of the AHC in FePt and FePd with the magnetization along [001] ( $\sigma_z$ ) and [100] ( $\sigma_x$ ). For each orientation,  $\sigma^{\uparrow\uparrow}$  ( $\sigma^{\uparrow\downarrow}$ ) is calculated by keeping only the first (second) term in the spin-orbit Hamiltonian (2), while both terms are kept when calculating of  $\sigma^{\text{tot}}$ .  $\Delta\sigma^{\uparrow\uparrow(\downarrow)}$  is defined as the difference between the spin-conserving (spin-flip) parts of  $\sigma_z$  and  $\sigma_x$ . All values are in S/cm.

metals [4]). The second mechanism involves spin-orbit driven transitions between bands with similar dispersion which are split in energy across the Fermi level. We shall refer to them as *ladder transitions*. Both occur at low frequencies, of the order of the spin-orbit coupling strength.

Let us briefly review the formalism for calculating the intrinsic AHC from first-principles. For a ferromagnet with the orthorhombic crystal structure and magnetization  $\mathbf{M}$  along the  $\hat{z}$  ([001]) axis, the AHC  $\sigma_z \equiv \sigma_{xy}$  is given by the  $k$ -space integral of the Berry curvature [1, 8]:

$$\sigma_z = \frac{e^2 \hbar}{4\pi^3} \text{Im} \int_{\text{BZ}} d\mathbf{k} \sum_{n,m}^{o,e} \frac{\langle \psi_{n\mathbf{k}} | v_x | \psi_{m\mathbf{k}} \rangle \langle \psi_{m\mathbf{k}} | v_y | \psi_{n\mathbf{k}} \rangle}{(\varepsilon_{m\mathbf{k}} - \varepsilon_{n\mathbf{k}})^2}. \quad (1)$$

In this expression,  $\psi_{n\mathbf{k}}$  and  $\psi_{m\mathbf{k}}$  are respectively the occupied ( $o$ ) and empty ( $e$ ) one-electron spinor Bloch eigenstates of the crystal with eigenvalues  $\varepsilon_{n\mathbf{k}}$  and  $\varepsilon_{m\mathbf{k}}$ ,  $v_x$  and  $v_y$  are Cartesian components of the velocity operator, and the integral is over the Brillouin zone (BZ). When the direction of  $\mathbf{M}$  is changed from the  $\hat{z}$ -axis to the  $\hat{x}$ -axis ([100]), the  $\sigma_x \equiv \sigma_{yz}$  component of the conductivity tensor should be calculated instead, by replacing  $v_x \rightarrow v_y$  and  $v_y \rightarrow v_z$  in Eq. (1).

The calculations were done using the approach of Ref. [11], whereby the linear-response expression (1) is rewritten in the basis of Wannier functions spanning the occupied and low-lying empty states. In this way the infinite sums over bands are replaced by sums over the small number of Wannier-interpolated bands. The Wannier functions were generated with WANNIER90 [12] using the same parameters as in Ref. [10], by post-processing first-principles calculations done using the Jülich density-functional theory FLAPW code FLEUR [13] (see Ref. [14] for details). The unit cell of FePt and FePd contained two atoms in the  $L1_0$  structure, with stacking along the [001]-direction. We used the generalized gradient approximation lattice constants of  $a = 5.14$  bohr and  $c = 7.15$  bohr for FePt, and  $a = 5.12$  bohr and  $c = 7.15$  bohr for FePd.

The atomic spin-orbit term in the Hamiltonian has the

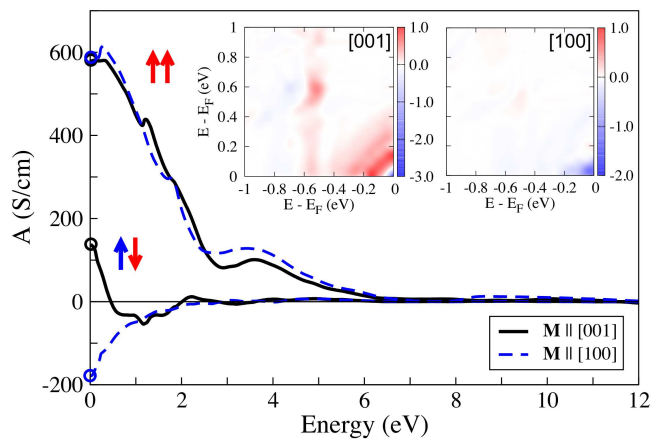


FIG. 1: (color online) Cumulative contribution to the AHC of FePt from the spin-flip ( $\uparrow\downarrow$ ) and spin-conserving ( $\uparrow\uparrow$ ) dichroic spectra above energy  $\omega$ . The values of AHC from Table I are indicated as open circles. The two insets display  $\Sigma^{\uparrow\downarrow}(E_v, E_c)$ , the energy-energy density of contributions to  $\sigma^{\uparrow\downarrow}$ , for  $\mathbf{M}$  along [001] and [100] (in  $10^5$  a.u./eV $^2$ ).

form

$$\xi \mathbf{L} \cdot \mathbf{S} = \xi L_{\hat{n}} S_{\hat{n}} + \xi (L_{\hat{n}}^+ S_{\hat{n}}^- + L_{\hat{n}}^- S_{\hat{n}}^+) / 2, \quad (2)$$

where  $\xi$  is the spin-orbit coupling strength,  $\hat{n}$  is the spin magnetization direction (which is taken as the spin-quantization axis),  $\mathbf{L}$  and  $\mathbf{S}$  are the orbital and spin angular momentum operators,  $L_{\hat{n}} = \mathbf{L} \cdot \hat{n}$ , and  $L_{\hat{n}}^+$  and  $L_{\hat{n}}^-$  are the corresponding raising and lowering operators (analogously for spin). We shall refer to the first and second terms in Eq. (2) as the spin-conserving ( $LS^{\uparrow\uparrow}$ ) and spin-flip ( $LS^{\uparrow\downarrow}$ ) parts of the SOI. This terminology refers to the effect of acting with each of them on an eigenstate of  $S_{\hat{n}}$ . Accordingly, we define  $\sigma^{\uparrow\uparrow}$  and  $\sigma^{\uparrow\downarrow}$  as the AHC calculated from Eq. (1) after selectively removing  $LS^{\uparrow\downarrow}$  or  $LS^{\uparrow\uparrow}$  from Eq. (2). This is not an exact decomposition, but inspection of Table I shows that it is approximately valid, as  $\sigma^{\text{tot}} \approx \sigma^{\uparrow\uparrow} + \sigma^{\uparrow\downarrow}$ .

The importance of spin-flip transitions for the AHC of FePt can be seen by analyzing its dependence on the magnetization direction (Table I). If only the spin-conserving term in Eq. (2) is kept, the resulting AHC  $\sigma^{\uparrow\uparrow}$  changes by less than 2% from an average value of about 580 S/cm as  $\mathbf{M}$  is tilted from the  $\hat{z}$ -axis to the  $\hat{x}$ -axis. When the spin-flip term is also included, the AHC  $\sigma^{\text{tot}}$  becomes highly anisotropic, decreasing by a factor of two, or roughly 400 S/cm, between [001] and [100]. Keeping only the spin-flip part of the SOI reveals that it is indeed chiefly responsible for the large anisotropy, as  $\sigma^{\uparrow\downarrow}$  changes by more than 300 S/cm, from a positive value along [001] to a large negative value along [100]. Such significant AHC anisotropy can occur in uniaxial ferromagnetic crystals, and was previously found in hcp Co [15]. However, in hcp Co the anisotropy is caused by spin-conserving pro-

	Fe <sup>tot</sup>	Fe <sup>↑</sup>	Fe <sup>↓</sup>	Pt <sup>tot</sup>	Pt <sup>↑</sup>	Pt <sup>↓</sup>
[001]	-13.7	17.9	-26.8	848.0	541.0	282.3
[100]	210.0	253.6	-37.5	65.0	425.7	-360.6

TABLE II: AHC in FePt for two magnetization directions, resolved into spin-flip and spin-conserving contributions from the SOI on each atomic species. All values are in S/cm.

cesses. This is also the case for FePd, as seen in Table I, and we shall comment further on this point below.

The AHC can be resolved in energy by defining a *cumulative* AHC  $A(\omega)$ , which accumulates all transitions in Eq. (1) for which  $\varepsilon_{m\mathbf{k}} - \varepsilon_{n\mathbf{k}} > \omega$  [15]. In the limit  $\omega \rightarrow 0$  all interband transitions in Eq. (1) are accounted for, and therefore  $A(\omega \rightarrow 0)$  equals the full intrinsic AHC. The spin-conserving and spin-flip cumulative AHCs are plotted in Fig. 1 in the range  $0 \leq \omega \leq 12$  eV, for both  $\mathbf{M} \parallel \hat{z}$  and  $\mathbf{M} \parallel \hat{x}$ . While  $A^\uparrow(\omega)$  remains largely isotropic over the entire energy range and decays rather slowly with  $\omega$  up to 4–5 eV in energy,  $A^\downarrow(\omega)$  picks up only for  $\omega$  below 1 eV and immediately becomes strongly anisotropic with decreasing energy, displaying a characteristic bifurcation shape [15]. Thus, the anisotropy in the AHC arises from spin-flip transitions within an energy window of about 0.5 eV around  $E_F$ .

In order to get further insight into the energy distribution of the spin-flip transitions, we define a new quantity  $\Sigma^\downarrow(E_v, E_c)$  as the contribution to  $\sigma^\downarrow$  from vertical transitions between pairs of states with energies in the vicinity of  $E_v < E_F$  and  $E_c > E_F$ . Thus,  $\iint \Sigma^\downarrow(E_v, E_c) dE_v dE_c = \sigma^\downarrow$ , and if the region of integration is restricted to  $E_c - E_v > \omega$ , we obtain  $A^\downarrow(\omega)$ .

The function  $\Sigma^\downarrow(E_v, E_c)$  is shown in the insets of Fig. 1 for the two magnetization directions. In both cases one can see intense blue dots near the origin. They denote large negative contributions concentrated at very low energies, arising from spin-orbit-induced avoided crossings between up- and down-spin Fermi-surface sheets. While for  $\mathbf{M} \parallel \hat{x}$  these hot-loop features are dominant, for  $\mathbf{M} \parallel \hat{z}$  a competing positive contribution can be clearly seen. It consists of a series of stripes  $E_c - E_v \approx \text{const.}$ , with the constant ranging from 0.1 to 0.5 eV. By analyzing the band structure we find that, owing to the off-diagonality of the  $LS^\downarrow$ -operator in the basis of localized  $d$ -orbitals, these transitions come from pairs of bands of different orbital character with similar dispersion on either side of  $E_F$ . Such ladder transitions, indicated schematically in the inset of Fig. 2, provide a different source of AHC. Compared to the hot loops, they do not require band crossings at the Fermi energy, and occur over wider ranges of energy and larger regions of  $k$ -space. In FePt with  $\mathbf{M} \parallel \hat{z}$  their contribution is so large that it wins over the hot-loop part and determines the sign and magnitude of  $\sigma^\downarrow$ .

The spin-flip processes in FePt are induced mostly by

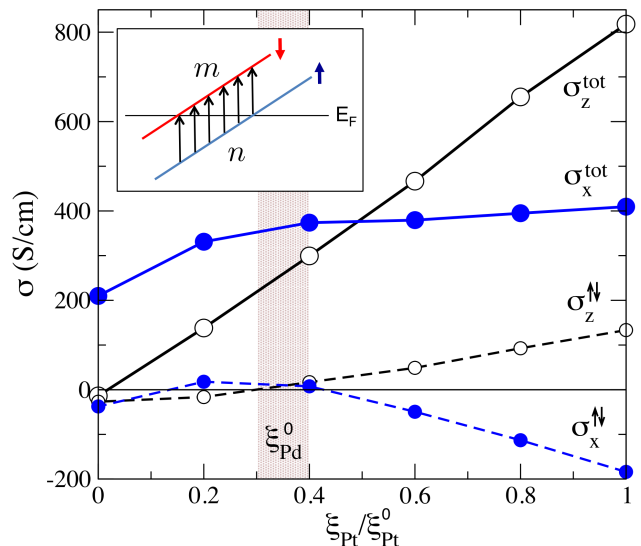


FIG. 2: (color online) Dependence of the total ( $\sigma_z^{\text{tot}}$  and  $\sigma_x^{\text{tot}}$ ) and spin-flip ( $\sigma_z^{\downarrow}$  and  $\sigma_x^{\downarrow}$ ) AHC in FePt alloy on the strength  $\xi_{\text{Pt}}$  of the SOI inside the Pt atoms. The inset depicts schematically the "ladder-type" spin-flip interband transitions.

the strong SOI on the Pt atoms. In order to prove this point, we have selectively turned off the SOI on each atomic species inside the crystal. The atom-resolved spin-orbit Hamiltonian reads

$$H^{\text{SO}} = \xi_{\text{Fe}} \mathbf{L}^{\text{Fe}} \cdot \mathbf{S} + \xi_{\text{Pt}} \mathbf{L}^{\text{Pt}} \cdot \mathbf{S}, \quad (3)$$

where  $\mathbf{L}^\mu$  is the orbital angular momentum operator associated with atomic species  $\mu$ , and  $\xi_\mu$  is the spin-orbit coupling strength averaged over valence  $d$ -orbitals. In FePt we find  $\xi_{\text{Fe}}^0 = 0.06$  eV and  $\xi_{\text{Pt}}^0 = 0.54$  eV, where  $\xi_\mu^0$  denotes the value calculated from first-principles.

We have recalculated the AHC after setting to zero either  $\xi_{\text{Fe}}$  or  $\xi_{\text{Pt}}$  in Eq. (3), and then using Eq. (2) to further decompose the remaining term. The results are presented in Table II. Although such a decomposition is not exact, it reproduces the results of Table I rather well. Namely, the sum of the total conductivities driven by SOI on Fe ( $\text{Fe}^{\text{tot}}$  in Table II) and on Pt ( $\text{Pt}^{\text{tot}}$  in Table II) is in reasonable agreement to the values of  $\sigma^{\text{tot}}$  from Table I for both magnetization directions. Moreover, the decomposition of the total atom-resolved AHCs into spin-conserving and spin-flip parts is almost exact, as can be seen from Table II.

Consider first the left part of the Table II, where the AHC is driven by  $\xi_{\text{Fe}}$ . For both magnetization directions the spin-flip contribution is very small, while the spin-conserving part is small along [001] but large along [100]. As for the AHC induced by  $\xi_{\text{Pt}}$ , shown on the right-side of the table, the spin-conserving part is large but fairly isotropic, while the spin-flip part is highly anisotropic, changing from a large positive value along [001] to a large

negative value along [100]. This confirms that the large and strongly anisotropic  $\sigma^{\uparrow\downarrow}$  is governed by the SOI inside the Pt atoms.

A large spin-flip contribution to the AHC in materials with strong spin-orbit coupling is perhaps not surprising, given that spin-flip transitions appear at second order in a perturbative treatment of the SOI. This is confirmed by nonperturbative calculations where we tune by hand the SOI strength  $\xi_{\text{Pt}}$  on the Pt atoms. The results for the total and spin-flip AHC are shown in Fig. 2 as a function of  $\xi_{\text{Pt}}/\xi_{\text{Pt}}^0$ . It can be seen that for  $\xi_{\text{Pt}}$  less than  $\xi_{\text{Pt}}^0/2$ , the absolute value of the spin-flip AHC does not exceed a modest value of 50 S/cm. In this regime  $\sigma_z^{\text{tot}}$  and  $\sigma_x^{\text{tot}}$  are dominated by spin-conserving processes. Moreover, we note that while the decrease in  $\sigma_z^{\text{tot}}$  is almost perfectly linear,  $\sigma_x^{\text{tot}}$  stays fairly constant over a wide region of  $\xi_{\text{Pt}}$  values. This can be understood from the fact that for  $\mathbf{M}||\hat{z}$  the spin-conserving and spin-flip contributions arising from  $\xi_{\text{Pt}}$  largely cancel one another (see Table II), so that the total AHC is mostly driven by the SOI on the Fe atoms. In contrast, for  $\mathbf{M}||\hat{x}$  it is the SOI on the Pt atoms which dictates the AHC.

The artificial tuning of  $\xi_{\text{Pt}}$  performed above describes rather well what happens if the Pt atoms are replaced with Pd, to form the experimentally known FePd alloy [10]. This can be seen by comparing the values of  $\sigma^{\text{tot}}$  and  $\sigma^{\uparrow\downarrow}$  for FePd in Table I with the values taken from the shaded area in Fig. 2, where  $\xi_{\text{Pt}} \approx \xi_{\text{Pd}}^0 = 0.19$  eV. In particular, the sign of the AHC anisotropy in FePd, which is opposite from that in FePt, is correctly reproduced by the scaled calculations on FePt.

In summary, we predict a large contribution from spin-flip transitions to the intrinsic AHE of FePt ordered alloys. Such transitions are induced by the strong spin-orbit interaction on the Pt atoms. They are concentrated at frequencies below the spin-orbit interaction energy, and their sign depends on the magnetization direction, making the AHE in this material strongly anisotropic. Our calculations have assumed perfectly ordered alloys, therefore neglecting extrinsic contributions to the AHC. First-principles methods capable of incorporating the effects of disorder in the calculation of the AHC have been recently developed [16-18]. An interesting direc-

tion for future work would be to use such methods to investigate both the role of spin-flip transitions and the orientation dependence of the extrinsic AHE.

We acknowledge discussions with M. Ležaić, Ph. Mavropoulos and K. M. Seemann. This work was supported by the HGF-YIG Programme VH-NG-513 and NSF Grant DMR-0706493. Computational time on JUROPA and JUGENE supercomputers was provided by Jülich Supercomputing Centre.

---

\* corresp. author: y.mokrousov@fz-juelich.de

- [1] N. Nagaosa, J. Sinova, S. Onoda, A. H. MacDonald and N. P. Ong, *Rev. Mod. Phys.* **82**, 1539 (2009)
- [2] J. E. Hirsch, *Phys. Rev. Lett.* **83**, 1834 (1999)
- [3] J. Shi, P. Zhang, D. Xiao and Q. Niu, *Phys. Rev. Lett.* **96**, 76604 (2006)
- [4] I. Žutić, J. Fabian and S. Das Sarma, *Rev. Mod. Phys.* **76**, 323 (2004)
- [5] C. Andersson, B. Sanyal, O. Eriksson *et al.*, *Phys. Rev. Lett.* **99**, 177207 (2007)
- [6] B. R. Cooper, *Phys. Rev.* **139**, A1504 (1965)
- [7] T. Naito, D. S. Hirashima and H. Kontani, *Phys. Rev. B* **81**, 195111 (2010)
- [8] Y. Yao, L. Kleinman, A. H. MacDonald *et al.*, *Phys. Rev. Lett.* **92**, 037204 (2004)
- [9] M. Chen, Z. Shi, S. M. Zhou *et al.*, arXiv:1004.0548v4 (2010)
- [10] K. M. Seemann, Y. Mokrousov, A. Aziz *et al.*, *Phys. Rev. Lett.* **104**, 076402 (2010)
- [11] X. Wang, J. R. Yates, I. Souza and D. Vanderbilt, *Phys. Rev. B* **74**, 195118 (2006)
- [12] A. A. Mostofi, J. R. Yates, Y.-S. Lee *et al.*, *Comp. Phys. Comm.* **178**, 685 (2008)
- [13] For description of the code see <http://www.flapw.de>
- [14] F. Freimuth, Y. Mokrousov, D. Wortmann *et al.*, *Phys. Rev. B* **78**, 035120 (2008)
- [15] E. Roman, Y. Mokrousov and I. Souza, *Phys. Rev. Lett.* **103**, 097203 (2009)
- [16] A. A. Kovalev, J. Sinova and Y. Tserkovnyak, *Phys. Rev. Lett.* **105**, 036601 (2010)
- [17] S. Lowitzer, D. Ködderitzsch and H. Ebert, *Phys. Rev. Lett.* **105**, 266604 (2010)
- [18] M. Gradhand, D. V. Fedorov, P. Zahn and I. Mertig, *Phys. Rev. Lett.* **104**, 186403 (2010)